PERFORMANCE DEMONSTRATION OF THE NON-INVASIVE BUNCH SHAPE MONITOR AT GSI HIGH CURRENT LINAC*

B. Zwicker, C. Dorn, P. Forck, O. Kester, P. Kowina, T. Sieber, GSI, Darmstadt, Germany

Abstract

At the heavy ion LINAC at GSI, a novel scheme of a non-invasive Bunch Shape Monitor has been tested with several different ion beams at 11.4 MeV/u and beam currents in the range from 80 to 1000 µA. Caused by the beam impact on the residual gas, secondary electrons are liberated. These electrons are accelerated by an electrostatic field, transported via a sophisticated electrostatic energy analyzer and an rf-deflector, acting as a time-to-space converter. Finally a MCP amplifies the electrons and the electron distribution is detected by a CCD camera. For the applied beam settings this Bunch Shape Monitor is able to obtain longitudinal profiles down to 250 ps RMS width with a resolution of 34 ps, corresponding to 0.5° of the 36 MHz accelerating frequency. Systematic parameter studies for the device were performed to demonstrate the applicability and to determine the achievable resolution. The background contributions, as originated by x-rays, are investigated.

MOTIVATION

Within the FAIR-Project [1] a proton LINAC [2] is scheduled as a new injector for the SIS18 synchrotron at GSI. The p-LINAC will provide 70 MeV and 70 mA current in addition to a compact construction. Due to the high energy deposition for conventional intersecting Bunch Shape Monitors [3, 4] a novel design is foreseen. The new detector for the longitudinal bunch structure with a phase resolution of 1°, with respect to the 325 MHz acceleration frequency, is intended to ensure proper longitudinal matching of the accelerating structures. The presented device is a recommissioning of the non-intercepting Bunch Shape Monitor presented in [5].

WORKING PRINCIPLE

The non-invasive Bunch Shape Monitor (BSM) prototype is based on secondary electrons, which are freed by the interaction of beam ions and the residual gas. Figure 1 provides a schematic illustration. These electrons are accelerated towards an aperture by an external homogeneous electrostatic field of 4.2 kV/mm. Using side strips parallel to the electrodes the electric field is leveled. To further reduce the divergence of the secondary electrons (SEs) two apertures with a distance of 70 mm are used. The aperture width can be remotely adjusted between 0.1 mm and 2 mm. After passing these apertures the electrons are filtered by two 90° cylindrical electrostatic energy analyzers with a bending radius of 30 mm. Two similar analyzers are used to bend the SE beam back in original direction for mechanical reasons.
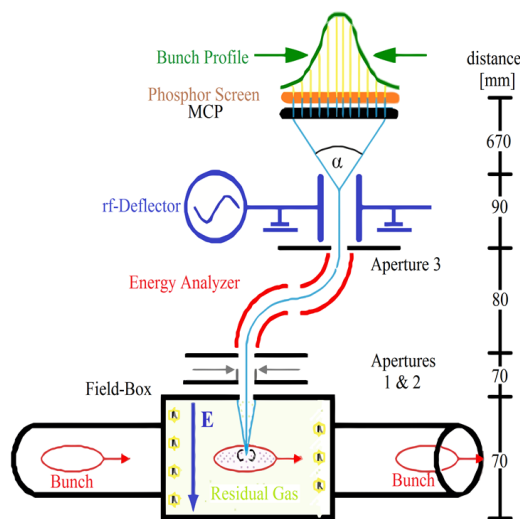
Figure 1: Schematic illustration of the non-invasive BSM

The applied voltages are ±5.5 kV for the opposite cylinder segments. A third aperture is placed 10 mm away from the edge of the second analyzer to enable a point-to-point focusing from the entrance to the exit slit. After a drift of 90 mm the SEs reach a radio frequency (rf) driven deflector coupled to the accelerating frequency. The rf-deflector works as a time-to-spatial converter. Each electron is deflected in dependence to its time of arrival. Two deflectors with different resonance frequencies are available. One is operating at a frequency of 36 MHz for long bunches and the other one for short bunches at the third harmonic at 108 MHz. Both deflectors are 800 mm long parallel wires corresponding to $\lambda/4$ for high field strength. The maximum power applicable is 100 W at 36 MHz and 50 W at 108 MHz in pulses of 6 ms duration. The deflected SEs, after a 670 mm flight, are spatially detected by a Chevron MCP (Hamamatsu F2226-24P) with an effective diameter of 77 mm and finally monitored by a P20 phosphor screen. The illuminated spots on the phosphor screen are observed by a CCD camera (PCO 12 Bit SensiCam, CCD chip of 640×480 pixel). In addition, the deflector has a second function as a focusing electrostatic einzel-lens by a common DC-voltage of maximal 6000 V on the deflector's plates. Between the rf-deflector and the MCP a 1 cm thick stainless steel plate is inserted as a x-ray shield for the MCP detector.

COMPENSATION OF THE BEAM DEFLECTION

While operating the BSM the applied E-Field affects the ion beam. For an 11.4 MeV U^{28+} beam with an applied voltage of -31 kV (resulting in a field strength of 420 V/mm) the

beam deflection is about 140 µrad according to CST based calculations, for a proton beam it is higher with 400 µrad. The present monitor location at UNILAC leads to a typical 50 % beam loss at the entrance of SIS18 at GSI facility, due to over stressing the synchrotron's acceptance. For a fore-seen operation within a LINAC the beam deflection must be minimized. Compensation electrodes have been built and designed. It was mandatory to upgrade the device without changing the existing vacuum chamber. The design of appropriate compensation requires a field simulation by CST finite elements code shown in Fig. 2.

Due to the lack of available insertion space (two thirds occupied by the Field-Box), the optimal design for complete compensation is not an option. Best suited is an identical Field-Box with opposite polarity, split it into equal halves and put in front and behind of the original Field-Box. This approach requires not available space, but with the help of a CST based simulation a more sophisticated design was chosen, which stays as close as possible with this solution and achieves sufficient compensation. Finally the selected design is a product of contrary objectives, achieving sufficient homogeneous high field strength with a fixed voltage of -31 kV and avoiding any material in a symmetry axis coaxial to the beam axis, at least 55 mm in diameter (iris size in front of the BSM). Capacitor plates with fixed distance are here inapplicable. In order to achieve a necessary field strength of 620 V/mm in comparison to 420 V/mm of the Field-Box a distance of maximum 50 mm is needed. To avoid material within the 55 mm safety buffer zone the capacitor plates are bent in the middle with a 60 mm diameter (see Fig. 2). Also for E-field leveling purposes electrode lamellas are attached at the fringes of the capacitor. The compensation f of the
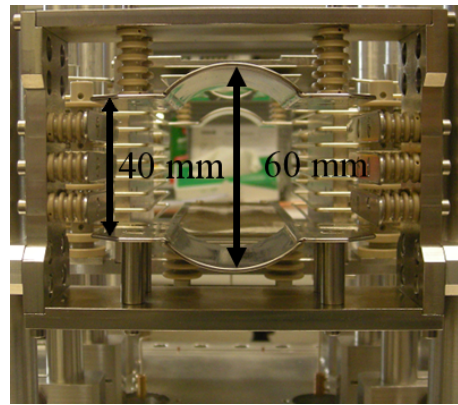

Figure 3: One of two compensation capacitors with its bended 60 mm opening. The polarity is swapped by applying the voltage to the upper plate instead of the lower one like the Field-Box does.

beam deflection is calculated with Equation (1).

$$f = \frac{\int E_y \,(\text{compensated}) \cdot dz}{\int E_y \,(\text{un-compensated}) \cdot dz} \qquad (1)$$

Along a beam path the field components for the compensated and non-compensated case are integrated, then the quotient f of both integrals is formed. The results for different beam paths are represented in Fig. 4 as a contour plot. According to the results a deflection of 48 µrad within a 50 mm diameter is still present for a 11.4 MeV proton beam and 17 µrad for a U^{28+} beam at the same energy per nucleon. The majority of the ion beam trajectories are sufficiently compensated. Beam based tests showed no detectable deflection or beam loss at the GSI synchrotron by using Beam Position Monitors.

EXAMPLE OF BUNCH SHAPE MEASUREMENTS

Using the BSM different bunch shapes were determined ranging from 1531 ps RMS down to 240 ps RMS. An example for the image of the MCP detector is depicted in Fig. 5.
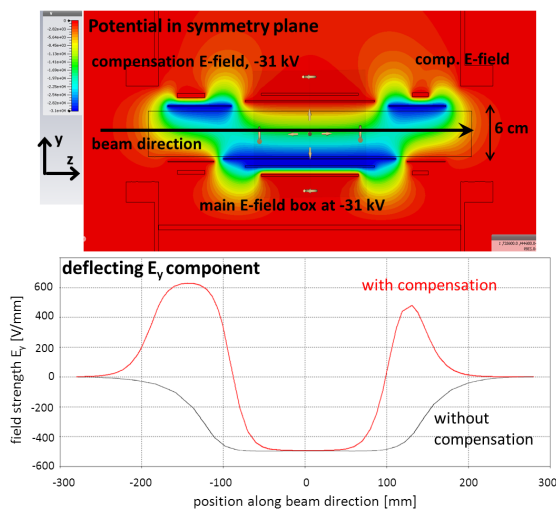

Figure 2: The upper image shows a CST finite element code based calculation of the potential distribution of the Field-Box inside the symmetry plane along the beam axis. The lower image shows the un-compensated and compensated E_y-field component along the beam axis.
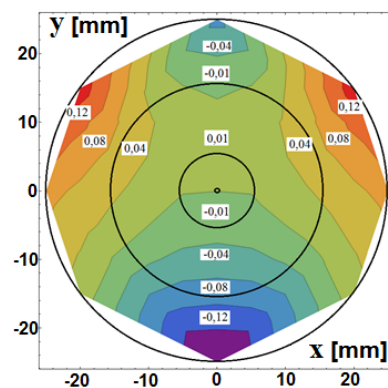

Figure 4: Contour plot of deflection in ion beam direction after compensation. Positive values indicate over compensation in relation to original value and direction.

The image is represented in pseudo colors to enhance contrast, while operating and adjusting the device. By projecting the spatial distribution over the axis of deflection the bunch shape including background is obtained. A second measurement is taken with identical setup besides the absence of the bunch signal by blocking the SEs with totally closed apertures. After equalizing the background level on both MCP images by averaging and comparing them at the fringe areas, where no bunch signal is expected, the background image can be subtracted from the other. The result of this procedure is also shown in Fig. 5.

To further proof the BSMs capabilities a measurement with different bunch shapes has been setup. By using a single gap resonator, mounted 60 m upstream of the monitor location, as a re-buncher for the beam with the right phase and sufficient strong amplitude, the bunch shape can be stretched or compressed. By systematical manipulation of the rf-amplitude inside the single gap resonator the longitudinal focal length can be varied and the bunch shape is modified. See Fig. 6 for the results of the measurement.
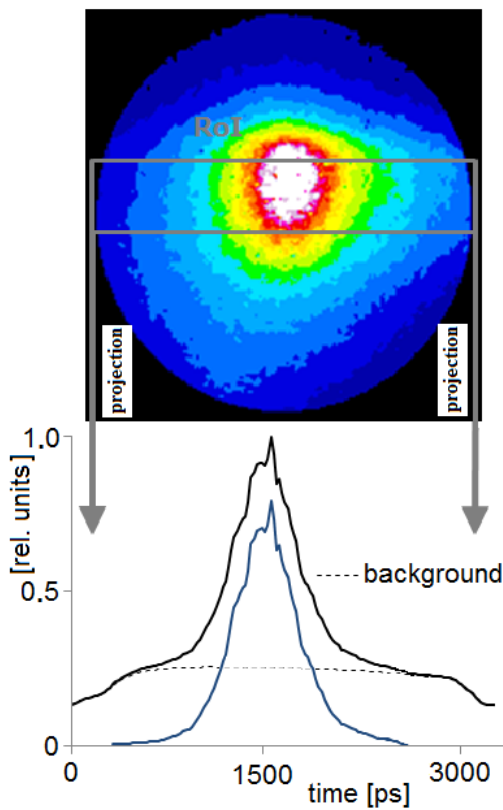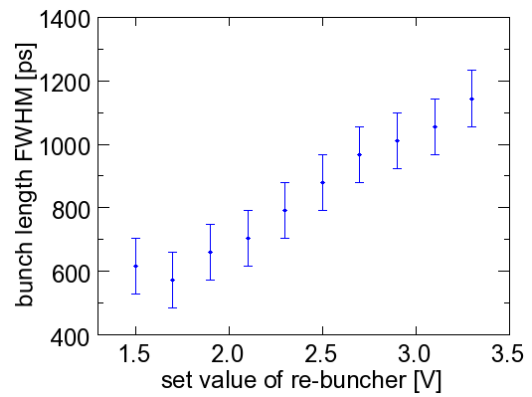

Figure 6: Bunch shape variation by the action of a re-buncher 60 m upstream of the BSM location. By varying the rf-amplitude of the re-buncher different bunch shapes from 570 ps FWHM to 1150 ps FWHM have been detected.

CALIBRATION PROCEDURE

In order to determine the longitudinal time structure of a bunch, a calibration has to be done and the resolution has to be determined [6]. The deflection angle and therefore the position of a detected electron depends on the amplitude and phase of the driving frequency of the rf-deflector. For a given amplitude the rf-phase is shifted by a preset degree corresponding to a certain time delay and regarding the displacement of the distribution, the phase calibration is done. In Fig. 7 the phase calibration is shown with a maximum of 100 W applied rf-power and the 36 MHz resonator. The high rf-power means broader spatial distributions and therefore allows to investigate more details with the same resolution. Depending on the bunch length, which might vary for different beam parameter settings, the rf-power can be varied

Figure 5: The MCP detector is shown in pseudo colors. By performing a projetion over the axis of deflection, a bunch structure, including background, is obtained. Furthermore, a background only measurement allows the substraction of the background. Parameters: RMS of 290 ps, Ni^{28+}, I = 900 μA, t_{pulse} = 180 μs, P = 5·10^{-6} mbar, 32 averages, phase calibration: 21 ps/pixel.
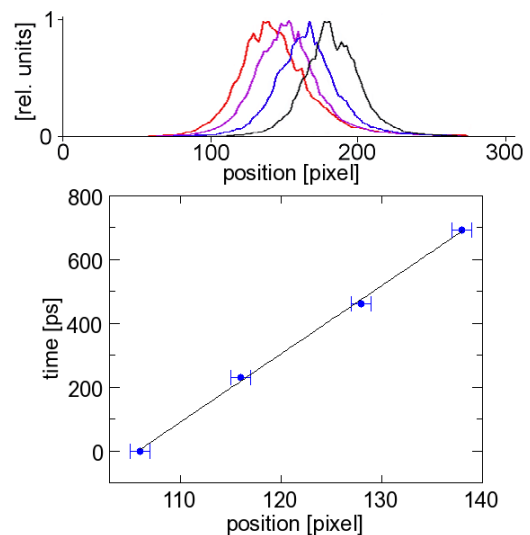

Figure 7: The upper image shows different measurements with 3° @ 36 MHz phase shift. The lower image shows the center of distribution plotted over their position lead to a calibration of (21.3 ± 0.5) ps/pixel.

to match the image of the bunch to the MCP size, leading to an optimal resolution. For each rf-power setting a new calibration must be performed.

DETERMINATION OF RESOLUTION

With only DC voltage applied to the rf-deflector, working as an electrostatic einzel-lens, the image properties can be investigated. Figure 8 shows a determination of the focus width and the corresponding voltage. With an aperture setup of 0.5 mm, 1 mm respectively, a minimum RMS of 0.6 mm was achieved. With a pixel width of 0.45 mm the total resolution is about 25 ps RMS for the rf-power as used for Fig. 7.

BACKGROUND INVESTIGATION

For further improvements of the BSM the source of the background was investigated. Here we refer to a background, which is statistically distributed over the entire MCP area and can therefore not be caused directly by the SE from the interaction of the beam and the residual gas. As a first step the residual gas pressure is varied from $5 \cdot 10^{-8}$ to $5 \cdot 10^{-6}$ mbar and determine the signal level for the entire area of the MCP. The apertures are closed to exclude SE contribution. Figure 9 shows a linear correlation between the pressure and the average background level for the attainable pressure range of $p \geq 5 \cdot 10^{-8}$ mbar. From this we can conclude that the background is generated locally within less than ± 1 m around the BSM where the gas pressure is increased. It is not originated by beam losses in this area which would be independent of the gas pressure. The intensity within the bunch image is averaged and shown in terms of signal-to-noise ratio in Fig. 9. Even though the pressure is varied over about two orders of magnitude, the signal-to-background ratio varies only within a factor

Figure 9: Upper image: First measurement of the pressure contribution to the background. Over two magnitudes the distribution is in good agreement with a linear fit. Lower image: Signal-to-background ratio with open apertures showing a variation of only a factor of two over full range. Parameters: N^{7+}, I = 900 μA, t_{pulse} = 180 μs, 20.5 kV driving potential, MCP = 1600 V, 16 averages, apertures closed for upper image.

of 2. From a second measurement, described in the next paragraph, we assign the main source of background to x-rays generated in the E-field.

To confirm the presence of x-rays, the applied voltage to the E-field box was varied from 2 kV to 30 kV. The background, distributed statistically on the entire MCP area, grows for increasing voltages as shown in Fig. 10. This is interpreted in terms of x-rays for the following reason: The interaction of the beam and the residual gas leads to electrons, which are accelerated towards a slit and energy analyzer by the applied field (top side in Fig. 1). But only a very small fraction is transmitted through the slits, with
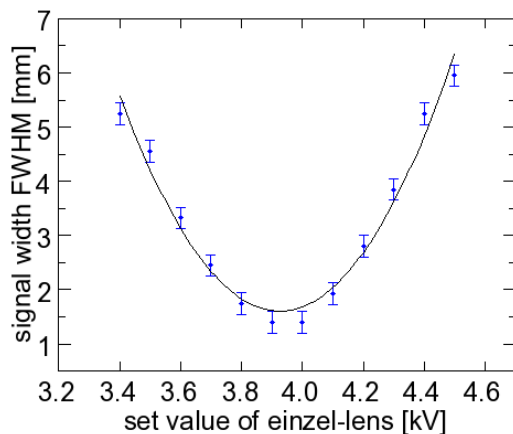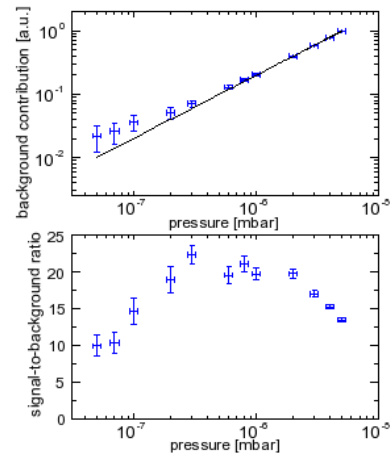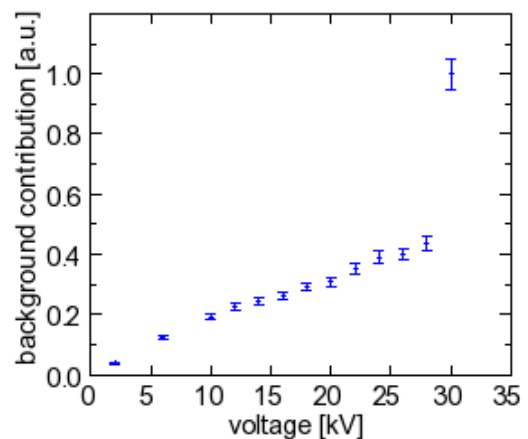

Figure 8: Focus width depending on the applied voltage on the einzel-lens, the solid line is a parabola fit. Parameters: Apertures 0.5 mm, 0.5 mm and 1 mm opened, 11.5 kV driving potential, 16 averages, $5 \cdot 10^{-6}$ mbar. The Field-Box bottom plate is used as SE source for higher intensity purposes.

Figure 10: Background (no SE contribution) increases with the applied voltage. Parameters: N^{7+}, I = 900 μA, t_{pulse} = 180 μs, $1 \cdot 10^{-6}$ mbar, MCP = 1600 V, 8 averages, apertures closed.

Beam Profile Monitors

Tuesday poster session

the majority of electrons hits the metal plate of the box and potentially creates x-rays. Moreover, the residual gas ions are accelerated towards the negative biased plate (bottom plate in Fig. 1) and by hitting the bottom plate secondary electrons are emitted for the surface, which are then accelerated toward the top plate of the E-field box. These electrons are accelerated by the full potential and finally they create additional x-rays when hitting the top plate. X-rays created by this effect seem to be the dominate source for the background, because the creation probability and the x-ray energy depends on the electron's kinetic energy, which is given by the applied voltage. This conclusion is supported by the fact that the signal-to-background ratio is basically independent from vacuum pressure, see Fig. 9. To suppress a large part of the electrons liberated by the residual gas ions, a grid is mounted close to the bottom electrode with a transmission of 90 % and biased to a proper potential of 3.44 kV between the grid and the ground plate. Further investigations have been performed and the analysis of the recorded data is ongoing.

SUMMERY AND OUTLOOK

A novel device for bunch shape measurement was tested in detail concerning its application at the high current ion LINAC and can be used with some modification at the FAIR proton LINAC:

- The non-invasive BSM has performed high quality measurements for the longitudinal bunch profile from 1200 ps RMS down to 240 ps RMS.
- Shorter bunches can potentially be resolved because the rf resolution for high rf-power can be chosen to be about 25 ps corresponding to 0.5° of the 36 MHz acceleration frequency. It is an advantage of the used technology that the resolution can be chosen with the help of the rf-power and the aperture settings.
- The background was investigated; it is caused by x-rays created by the secondary electrons or further electrons caused by the residual gas ion impact on the HV bottom plate. For a bunch length determination with sufficient averages, this over the entire MCP-detector statistically distributed background can reliably be sub-

tracted. However a better shielding of the MCP-detector has to be installed.
- The related signal-to-background ratio is more than sufficient for a reliable bunch length determination with an adequate resolution and enables good statistics with only 16 averages per profile measurement. Therefore the acquisition time decreases below one minute.
- For the FAIR proton LINAC a higher deflection frequency of 325 MHz will be used. The achieved phase resolution of 0.5° will be preserved i.e. a required time resolution of 10 ps or less.

ACKNOWLEDGMENT

REFERENCES

[1] O. Kester, "Status of the FAIR Facility," IPAC'13, Shanghai, May 2013, TUXB101, p. 1085, `http://www.JACoW.org`

[2] L. Groening et al., "Status of the FAIR 70 MeV Proton Linac," LINAC'12, Tel-Aviv, September 2013, THPB034, p. 927, `http://www.JACoW.org`

[3] A. Feschenko, "Technique and Instrumentation For Bunch Shape Measurements", RuPAC'12, Saint-Petersburg, September 2012, FRXOR01, p. 181, `http://www.JACoW.org`

[4] A. Feschenko et al., "Bunch Shape Monitors With RF Scanning of Low Energy Secondary Electrons," Workshop on Bunch Shape Measurment, Lund, February 2013. `https://indico.esss.lu.se/indico/contributionDisplay.py?contribId=1&confId=44`

[5] P. Forck et al., "Measurements with a Novel Non-intercepting Bunch Shape Monitor at the High Current GSI-LINAC," DIPAC'05, Lyon, June 2005, POM010, p. 48, `http://www.JACoW.org`

[6] B. Zwicker et al., "Test of a Non-Invasive Bunch Shape Monitor at GSI High Current LINAC," IBIC'13, Oxford, September 2013, MOPC36, `http://www.JACoW.org`